LBL-37881
UC-414
Preprint

Lawrence Berkeley Laboratory

UNIVERSITY OF CALIFORNIA

Physics Division

Submitted to Zeitschrift für Physik C

The $\overline{\mathrm{MS}}$ Renormalized Bottom Mass of Order $\mathcal{O}(\alpha_s G_F M_t^2$ and Its Application to $\Gamma(H \to b\bar{b})$

A. Kwiatkowski and M. Steinhauser

October 1995

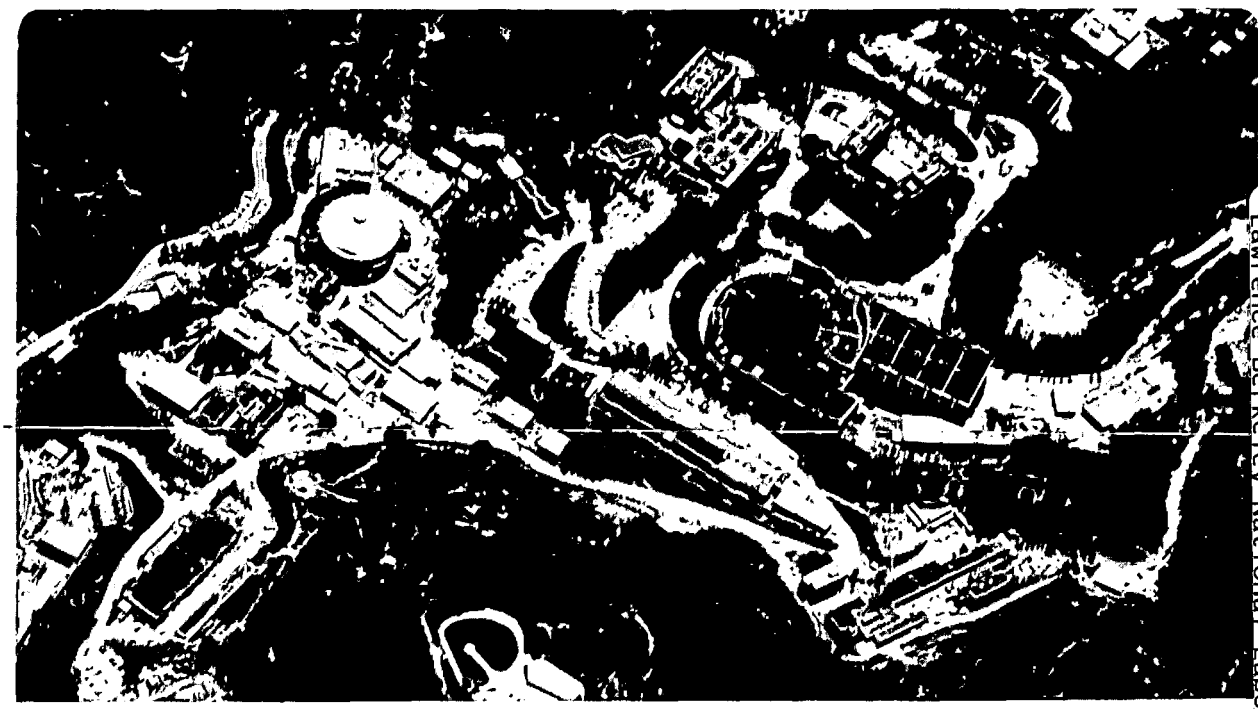

REFERENCE COPY
Does Not
Circulate
Bldg. 50 Library - Ref.
Lawrence Berkeley National Laboratory
LBL-37881
Copy 1

Prepared for the U.S. Department of Energy under Contract Number DE-AC03-76SF00098

DISCLAIMER

This document was prepared as an account of work sponsored by the United States Government. While this document is believed to contain correct information, neither the United States Government nor any agency thereof, nor the Regents of the University of California, nor any of their employees, makes any warranty, express or implied, or assumes any legal responsibility for the accuracy, completeness, or usefulness of any information, apparatus, product, or process disclosed, or represents that its use would not infringe privately owned rights. Reference herein to any specific commercial product, process, or service by its trade name, trademark, manufacturer, or otherwise, does not necessarily constitute or imply its endorsement, recommendation, or favoring by the United States Government or any agency thereof, or the Regents of the University of California. The views and opinions of authors expressed herein do not necessarily state or reflect those of the United States Government or any agency thereof or the Regents of the University of California.

LBNL–37881
TTP 95–35*
hep-ph/9510456
October 1995

The $\overline{\mathrm{MS}}$ Renormalized Bottom Mass of Order $\mathcal{O}(\alpha_s G_F M_t^2)$ and its Application to $\Gamma(H \to b\bar{b})$†

A. Kwiatkowski[a‡] M. Steinhauser[b]

[a] Theoretical Physics Group
Lawrence Berkeley National Laboratory
University of California
Berkeley, CA. 94720, USA

[b] Institut für Theoretische Teilchenphysik
Universität Karlsruhe
D-76128 Karlsruhe, Germany

Abstract

The renormalized mass of the bottom quark is calculated at the two loop level to order $\mathcal{O}(\alpha_s G_F M_t^2)$ in the $\overline{\mathrm{MS}}$ renormalization scheme. Different strategies for the computation are outlined. The result is applied to the partial decay rate $\Gamma(H \to b\bar{b})$ of the Higgs boson into bottom quarks. Expressing the width in terms of the running mass instead of the bottom pole mass allows to treat the $\mathcal{O}(\alpha_s G_F M_t^2)$ radiative corrections on the same footing as is commonly used in pure QCD calculations. The numerical values for the corrections are given and the sizes of different contributions are compared.

*The complete postscript file of this preprint, including figures, is available via anonymous ftp at ttpux2.physik.uni-karlsruhe.de (129.13.102.139) as /ttp95-35/ttp95-35.ps or via www at http://ttpux2.physik.uni-karlsruhe.de/cgi-bin/preprints/ Report-no: TTP95-35 and at http://theor1.lbl.gov/www/theorgroup/papers/37881.ps.

†This work was in part supported by US DoE under Contract DE-AC03-76SF00098.

‡Supported by Deutsche Forschungsgemeinschaft, grant no. Kw 8/1-1.

1 Introduction

Studying the properties of the Higgs boson, once it is discovered in future particle accelerators, will be the prime tool to experimentally probe the details of the electroweak symmetry breaking mechanism in the Standard Model. Of particular interest will be the Higgs boson decay into bottom quarks, since the decay channel $H \to b\bar{b}$ dominates in the intermediate Higgs mass range $M_H < 2M_W$. This process will be even more important, if possible hints for new physics effects in the reported descrepancy [1] between the measured partial Z boson width R_b into bottom quarks and its theoretical prediction should happen to substantiate. Similar effects might then also be visible in Higgs decays $H \to b\bar{b}$ and emphasize the need for precise Standard Model predictions to $\Gamma(H \to b\bar{b})$.

As a consequence much work has been spent on the calculation of radiative corrections to Higgs processes in the past and excellent reviews on Higgs phenomenology can be found in the literature [2, 3]. Previous works concerning the partial rate $\Gamma(H \to b\bar{b})$ include electroweak one loop corrections [4, 5, 6], the calculations of universal and nonuniversal corrections of the order $\mathcal{O}(\alpha_s G_F M_t^2)$ [7, 8, 9, 10], and recently even a three loop $\mathcal{O}(\alpha_s^2 G_F M_t^2)$ calculation was presented [11, 12]. Nonuniversal corrections to the vertex $Hb\bar{b}$ involve the virtual top quark through Higgs ghost exchange. Their top mass enhancement $\propto m_t^2$ due to Yukawa couplings distinguishes them from similar vertices of the Higgs boson to other quark flavours.

In our earlier work [9] the diagrams of Figure 1 were considered in the heavy top limit $M_t^2 \gg M_H^2$. The two loop $\mathcal{O}(\alpha_s G_F M_t^2)$ relation between the bare mass m_0 and the on-shell (OS) mass M_b of the bottom quark was presented and the corrections to the partial Higgs width were expressed in terms of M_b.

The $\overline{\text{MS}}$ renormalization scheme on the other hand is the commonly used renormalization prescription in higher order QCD calculations. Apart from calculational convenience its concept of the running bottom mass $\bar{m}_b$ allows the absorption of large logarithms $\ln(M_b^2/M_H^2)$ (see e.g. [13, 14, 15, 16]) and causes the perturbation series to converge more rapidly than in the OS scheme. It is therefore of obvious interest to adopt the notion of the running $\overline{\text{MS}}$ mass $\bar{m}_b$ in the Higgs decay rate also for the case when electroweak corrections are included.

For this reason we have calculated the two loop relation of order $\mathcal{O}(\alpha_s G_F M_t^2)$ between the on-shell mass and the $\overline{\text{MS}}$ renormalized mass of the bottom quark (for a discussion at the one loop level see [17]). This transformation from one renormalization scheme to the other allows to express $\Gamma(H \to b\bar{b})$ to the order $\mathcal{O}(\alpha_s G_F M_t^2)$ throughout in terms of the running mass $\bar{m}_b$.

The problem is approached in four different ways. All methods are leading to the same answer and thus provide powerful crosschecks beyond the standard consistency checks such as gauge invariance.

In order to introduce our notation let us start from the bare Lagrangian and consider

the bare fermion propagator for the bottom quark

$$S_0^{-1} = i(m_0 - \not{p} - m_0\Sigma_S^0 - \not{p}\Sigma_V^0). \tag{1}$$

We have not written the term $\not{p}\gamma_5\Sigma_A^0$ for notational simplicity, since for all quark mass relations below Σ_A becomes relevant only in higher order electroweak corrections $\mathcal{O}(G_F^2)$, which we do not consider in this work. We quote our previous result for the $\mathcal{O}(\alpha_s G_F M_t^2)$ bottom pole mass

$$M_b = m_0 \frac{1 - \Sigma_S^0}{1 + \Sigma_V^0}. \tag{2}$$

in Eq.(26) of the appendix, where for later convenience Σ_S^0 and Σ_V^0 are expressed in terms of the $\overline{\text{MS}}$ masses $\bar{m}_b$ and $\bar{m}_t$.

By rescaling its parameters the bare Lagrangian can be written as the sum of the renormalized Lagrangian and the counterterm Lagrangian. Our interest focuses on the renormalization constants Z_2 and Z_m relating the bare wavefunction and mass of the bottom quark to their renormalized equivalents

$$\Psi_0 = Z_2^{1/2}\Psi, \quad m_0 = Z_m \bar{m}_b. \tag{3}$$

Here we adopt the $\overline{\text{MS}}$ renormalization scheme as is indicated through bars. The renormalized bottom quark propagator accordingly reads

$$\begin{aligned} S_R^{-1} &= Z_2 S_0^{-1} \\ &= i\Big(\bar{m}_b - \not{p} - \bar{m}_b\bar{\Sigma}_S - \not{p}\bar{\Sigma}_V + (Z_2 Z_m - 1)\bar{m}_b - \not{p}(Z_2 - 1)\Big) \end{aligned} \tag{4}$$

For the determination of the $\overline{\text{MS}}$ bottom mass we perform our calculations according to the following different strategies.

In Section 2.1 the overall counterterms $\bar{\Sigma}_S^{CT}, \bar{\Sigma}_V^{CT}$ to the bottom selfenergy are computed in the $\overline{\text{MS}}$ scheme. With

$$\begin{aligned} Z_2 &= 1 - \bar{\Sigma}_V^{CT} \\ Z_2 Z_m &= 1 + \bar{\Sigma}_S^{CT} \end{aligned} \tag{5}$$

one obtains the relation between the $\overline{\text{MS}}$ and bare masses

$$\bar{m}_b = m_0 \frac{1 - \bar{\Sigma}_V^{CT}}{1 + \bar{\Sigma}_S^{CT}}. \tag{6}$$

In combination with Eq.(2) this leads to the transformation rule between OS- and $\overline{\text{MS}}$ masses of the bottom quark.

$$M_b = \bar{m}_b \frac{(1 + \bar{\Sigma}_S^{CT})(1 - \Sigma_S^0)}{(1 - \bar{\Sigma}_V^{CT})(1 - \Sigma_V^0)}. \tag{7}$$

In Section 2.2 a different approach is used to verify the findings of Section 2.1. The renormalized bottom quark propagator Eq.(4) is rewritten in the form

$$S_R^{-1} = i\left\{\bar{m}_b\left(1-\bar{\Sigma}_S+\bar{\Sigma}_S^{CT}\right)-\not{p}\left(1+\bar{\Sigma}_V-\bar{\Sigma}_V^{CT}\right)\right\} \tag{8}$$

with $\bar{\Sigma}_S = Z_2 Z_m \Sigma_S^0$, $\bar{\Sigma}_V = Z_2 \Sigma_V^0$. We check by explicit calculation of the finite parts of the bottom quarks self energies $\bar{\Sigma}_S^{fin}, \bar{\Sigma}_V^{fin}$ that the relation

$$\begin{aligned} M_b = & \ \bar{m}_b \frac{(1-\bar{\Sigma}_S+\bar{\Sigma}_S^{CT})}{(1+\bar{\Sigma}_V-\bar{\Sigma}_V^{CT})} \\ = & \ \bar{m}_b \frac{(1-\bar{\Sigma}_S^{fin})}{(1+\bar{\Sigma}_V^{fin})} \end{aligned} \tag{9}$$

is indeed equivalent to the prescription Eq.(7).

In Section 2.3 our problem is considered from a third point of view, which becomes transparent by expressing the renormalized quark propagator in the following form

$$S_R^{-1} = iZ_2\Big(Z_m\bar{m}_b - \not{p} - Z_m\bar{m}_b\Sigma_S^0 - \not{p}\Sigma_V^0\Big). \tag{10}$$

This expression is finite if the bare parameters in $\Sigma_{S,V}^0$ are substituted in favour of the renormalized ones. One therefore can solve for Z_2 and Z_m recursively, i.e. loop by loop. The renormalization constant Z_m leads then to the same result for $\bar{m}_b$ as in the previous sections.

Finally we demonstrate in Section 2.4 that another simple derivation of the result is possible, based on the earlier determination of the bottom pole mass and leading to the same $\bar{m}_b$ again.

The results are then applied in Section 3 to the partial decay rate $\Gamma(H \to b\bar{b})$. The numerical size of the corrections are given and the renormalization scheme dependence is discussed.

2 Calculation of the $\overline{\text{MS}}$ Renormalized Bottom Mass

2.1 Approach 1: Counterterms

We calculate the $\overline{\text{MS}}$ counterterms on a graph by graph basis in this section. Per definition of the $\overline{\text{MS}}$ scheme counterterm vertices consist of pole terms only and are therefore easier to compute than full diagrams. The integrals represented by the graphs in Figure 1 involve several mass scales. Via electroweak interactions the top quark and the Higgs ghost come into play with their respective scales M_t and M_W. In the heavy top limit $M_t^2 \to \infty$ one has $M_W^2 \ll M_t^2$. Since we consider only the leading term $\propto M_t^2$ in the power series of the

inverse top mass, one can neglect M_W right from the beginning. As a consequence the electroweak gauge parameter drops out trivially. The heavy mass expansion [18, 19, 20, 21] has developed into a well established technique and was sucessfully used in a number of applications. For a more detailed description the reader is referred for example to [22]. The main virtue of this method is the factorization of a multiloop integral containing the heavy top quark into an integral with less number of loops and massive tadpole integrals.

This decomposition is operative in our problem as well. Two loop integrals eventually factorize into a one loop tadpole and a one loop propagator integral, where the latter involves two scales, namely the bottom mass and the external momentum. However, being interested in the pole parts only, the matter simplifies even more. Since the pole terms are independent of masses and momenta, one can conveniently nullify either of them. Care must be taken that no spurious infrared divergencies are introduced in this way. In our case we have obtained the pole parts to Σ_S by setting the external momentum to zero, thus reducing the massive propagator integral to a tadpole integral. Similarly, for the computation of Σ_V the bottom mass is nullified. The resulting massless propagator integral is conveniently computed with the help of MINCER [23] which is based on the symbolic manipulation program FORM [24].

The counterterms of the one loop diagrams "QCD" and "EW" of Figure 1 are simply given by their pole terms obtained in the above described manner. On the two loop level the situation is somewhat more involved, since the diagrams "IN", "OUT" and "LEFT" contain ultraviolet divergent subgraphs. As is indicated in Figure 2, these subdivergences have to be subtracted in order to arrive at the overall divergence of the corresponding diagrams. The removal of the subdivergences results in local counterterm vertices, which we list in the appendix. It can be seen that indeed all logarithms have dropped out.

Whereas the counterterms are still gauge dependent, the QCD gauge parameter ξ_s cancels in the following expression for the bottom mass:

$$\begin{aligned} \bar{m}_b &= m_0 \frac{1-\bar{\Sigma}_V^{CT}}{1+\bar{\Sigma}_S^{CT}} \\ &= m_0 \left(1 + \frac{\alpha_s}{\pi}\frac{1}{\epsilon} + \bar{x}_t \frac{3}{2}\frac{1}{\epsilon} + \frac{\alpha_s}{\pi}\bar{x}_t \frac{2}{\epsilon}\right) \end{aligned} \tag{11}$$

with $\bar{x}_t = G_F \bar{m}_t^2 / 8\sqrt{2}\pi^2$. This leads to the transformation between the pole and the $\overline{\mathrm{MS}}$ mass of the bottom quark

$$\begin{aligned} M_b = \; & \bar{m}_b \; \frac{(1+\bar{\Sigma}_S^{CT})(1-\Sigma_S^0)}{(1-\bar{\Sigma}_V^{CT})(1-\Sigma_V^0)} \\ = \; & \bar{m}_b \; \left\{ 1 + \frac{\alpha_s}{\pi}\left(\frac{4}{3} + \ln\frac{\mu^2}{\bar{m}_b^2}\right) + \bar{x}_t \left(\frac{5}{4} + \frac{3}{2}\ln\frac{\mu^2}{\bar{m}_t^2}\right) \right. \\ & \left. + \frac{\alpha_s}{\pi}\bar{x}_t \left(\frac{9}{2} - 4\zeta(2) + \frac{5}{2}\ln\frac{\mu^2}{\bar{m}_t^2} + \frac{5}{4}\ln\frac{\mu^2}{\bar{m}_b^2} + \frac{3}{2}\ln^2\frac{\mu^2}{\bar{m}_t^2} + \frac{3}{2}\ln\frac{\mu^2}{\bar{m}_t^2}\ln\frac{\mu^2}{\bar{m}_b^2}\right)\right\}. \end{aligned} \tag{12}$$

2.2 Approach 2: Finite parts

As a cross check of the result Eq.(12) we now want to recalculate it in a different way, namely by employing only the finite parts of the corresponding bottom self energy graph as given in Eq.(9). The finite part of a diagram

$$\bar{\Sigma}^{fin}_{S,V} = \bar{\Sigma}^{full}_{S,V} - \bar{\Sigma}^{sub}_{S,V} - \bar{\Sigma}^{CT}_{S,V} \tag{13}$$

is obtained by subtracting the overall counterterm $\bar{\Sigma}^{CT}_{S,V}$ and the counterterm with the subdivergence $\bar{\Sigma}^{sub}_{S,V}$ from the full diagram $\bar{\Sigma}^{full}_{S,V}$. Pictorially this procedure is visualized in Figure 3. Notice that $\bar{\Sigma}^{sub}_{S,V}$ contains both pole and finite terms. One therefore cannot use the nullification procedure of the previous section to simplify the calculation.

Instead it is possible to simplify integrals by evaluating them on the mass shell $p^2 = M_b^2$ [25] using the expansion

$$\begin{aligned} \bar{\Sigma}^{full}_{S,V}\left(\frac{\bar{m}_b^2}{p^2}\right) &= \bar{\Sigma}^{full}_{S,V}(1) + \left(\frac{\bar{m}_b^2}{p^2} - 1\right)\bar{\Sigma}'_{S,V}(1) \\ &= \bar{\Sigma}^{full}_{S,V}(1) + 2\left(\bar{\Sigma}_S + \bar{\Sigma}_V\right)\bar{\Sigma}'_{S,V}(1). \end{aligned} \tag{14}$$

The derivatives $\bar{\Sigma}'_{S,V} \equiv \partial\bar{\Sigma}_{S,V}/\partial(\bar{m}_b^2/p^2)$ may be conveniently obtained through derivations with respect to $\bar{m}_b$, thus raising the power in the denominator of the integrand. This procedure may also be applied for the calculation of subdivergence counterterms, where the corresponding expansion reads

$$\bar{\Sigma}^{sub}_{S,V}\left(\frac{\bar{m}_b^2}{p^2}\right) = \bar{\Sigma}^{sub}_{S,V}(1) + 2\left(\bar{\Sigma}^{CT}_S + \bar{\Sigma}^{CT}_V\right)\bar{\Sigma}'_{S,V}(1). \tag{15}$$

The expressions for the finite parts of the various contributions are listed in the appendix. They lead to the relation between pole and $\overline{\mathrm{MS}}$ bottom mass

$$\begin{aligned} M_b = \; & \bar{m}_b \; \frac{(1-\bar{\Sigma}^{fin}_S)}{(1+\bar{\Sigma}^{fin}_V)} \\ = \; & \bar{m}_b \; \left\{1 + \frac{\alpha_s}{\pi}\left(\frac{4}{3} + \ln\frac{\mu^2}{\bar{m}_b^2}\right) + \bar{x}_t\left(\frac{5}{4} + \frac{3}{2}\ln\frac{\mu^2}{\bar{m}_t^2}\right)\right. \\ & \left. + \frac{\alpha_s}{\pi}\bar{x}_t\left(\frac{9}{2} - 4\zeta(2) + \frac{5}{2}\ln\frac{\mu^2}{\bar{m}_t^2} + \frac{5}{4}\ln\frac{\mu^2}{\bar{m}_b^2} + \frac{3}{2}\ln^2\frac{\mu^2}{\bar{m}_t^2} + \frac{3}{2}\ln\frac{\mu^2}{\bar{m}_t^2}\ln\frac{\mu^2}{\bar{m}_b^2}\right)\right\} \end{aligned} \tag{16}$$

We find agreement with Eq.(12).

2.3 Approach 3: Renormalization Constants

In our third method we proceed along a path which deals directly with the renormalization constants Z_2 and Z_m. To explain how both Z_2, Z_m are computed iteratively loop by loop,

it is convenient to consider the the renormalized fermion propagator in the following form:

$$S_R^{-1} = iZ_2\Big(Z_m\bar{m}_b - \not{p} - Z_m\bar{m}_b\Sigma_S^0 - \not{p}\Sigma_V^0\Big) \tag{17}$$

Here the bare bottom selfenergies $\Sigma_{S,V}^0 = \Sigma_{S,V}^{(1)0}(m_{b,0}, m_{t,0}) + \Sigma_{S,V}^{(2)0}(m_{b,0}, m_{t,0})$ receive contributions from the one and two loop diagrams of Figure 1. The explixcit arguments shall emphasize that all parameters are understood as bare quantities. In general the parameterlist would also include coupling constants, gauge parameters etc. If we now substitute the bare masses in favour of their renormalized counterparts at a given loop level, the functional form of the selfenergies does not change in that given order, but additional contributions of higher order are induced:

$$\Sigma_{S,V}^{(1)0}(m_{b,0}, m_{t,0}) = \Sigma_{S,V}^{(1)0}(\bar{m}_b, \bar{m}_t) + \Sigma_{S,V,\text{ind}}^{(2)} \tag{18}$$

Let us first consider the one loop case. Having expressed Eq.(17) entirely in terms of renormalized quantities, the renormalization constants Z_2, Z_m must be such that the inverse quark propagator is finite and, stated more precisely for the $\overline{\text{MS}}$ scheme, that the poles cancel. According to the Lorentz structure this results in two equations

$$\begin{aligned} \bar{m}_b Z_2 Z_m \left(1 - \Sigma_S^{(1)0}(\bar{m}_b, \bar{m}_t)\right) &\stackrel{!}{=} \text{finite} \\ \not{p} Z_2 \left(1 + \Sigma_V^{(1)0}(\bar{m}_b, \bar{m}_t)\right) &\stackrel{!}{=} \text{finite,} \end{aligned} \tag{19}$$

which can be solved for Z_2 and Z_m. The solution for Z_m leads to the one loop result for the $\overline{\text{MS}}$ mass $\bar{m}_b$.

The procedure can then be repeated for the two loop case. Besides the two loop result $\Sigma_{S,V}^{(2)0}$ also the induced second order terms $\Sigma_{S,V,\text{ind}}^{(2)}$ from the transition to the renormalized parameters at the one loop iteration have to be taken into account. Solving the corresponding system of equations gives the renormalization constants at the two loop level. Inversion of Eq.(3) with

$$Z_m = 1 - \bar{x}_t\frac{3}{2\epsilon} - \frac{\alpha_s}{\pi}\frac{1}{\epsilon} + \frac{\alpha_s}{\pi}\bar{x}_t\left(\frac{3}{\epsilon^2} - \frac{2}{\epsilon}\right). \tag{20}$$

indeed confirms the result Eq.(11).

2.4 Approach 4: Derivation from OS Mass

Having approached the problem from three different sides, let us demonstrate, how the $\overline{\text{MS}}$ bottom mass can be derived in another elegant manner. We start with the following ansatz for the relation between the bare mass and the $\overline{\text{MS}}$ mass of the bottom quark (a similar method was used in [26]) and insert it into Eq.(2):

$$M_b = \bar{m}_b\left\{1 + \frac{\alpha_s}{\pi}\frac{a}{\epsilon} + x_{t,0}\frac{b}{\epsilon} + \frac{\alpha_s}{\pi}x_{t,0}\left(\frac{c}{\epsilon^2} + \frac{d}{\epsilon}\right)\right\}\frac{1 - \Sigma_S^0}{1 + \Sigma_V^0} \tag{21}$$

The bare top mass in $x_{t,0}$ is substituted through the renormalized $\overline{\mathrm{MS}}$ mass and the terms following the curly bracket are taken from the pole mass calculation in Eq.(26).

The crucial step is to require that the pole mass M_b on the LHS as a physical quantity must be finite. This translates into the requirement that all coefficients of $1/\epsilon$ poles on the RHS must vanish. Thus one obtains four equations which can be solved for the unknown coefficients a, b, c, d. Two additional equalities follow from the fact that the logarithms of the pole terms cancel separately and serve as a consistency check for the solutions

$$a = -1, \quad b = -\frac{3}{2}, \quad c = 0, \quad d = -2. \tag{22}$$

Insertion into Eq.(21) produces again the result Eq.(12) and Eq.(16).

3 Application to the Higgs Decay $H \to b\bar{b}$

In this section we apply our result to the partial Higgs boson decay rate [9, 10]

$$\Gamma(H \to b\bar{b}) = \Gamma_0 M_b^2 \left\{ 1 + X_t + \frac{\alpha_s}{\pi} X_t \left(-1 - 4\zeta(2) - 2\ln\frac{M_H^2}{M_b^2} \right) \right\} \tag{23}$$

where $\Gamma_0 = 3G_F M_H/4\sqrt{2}\pi$, $X_t = G_F M_t^2/8\sqrt{2}\pi^2$ and the renormalization scale is chosen as $\mu^2 = M_H^2$. For our following numerical discussion we use as input values a bottom pole mass of $M_b = 4.7$ GeV and a top mass of $M_t = 176$ GeV. Based on $\Lambda_{QCD}^{(5)} = 233$ MeV the running strong coupling constant ranges between $\alpha_s(M_H = 70 \text{ GeV}) = 0.125$ and $\alpha_s(M_H = 130 \text{ GeV}) = 0.114$ where $\alpha_s(\mu)$ is defined for five active flavours. We now express the above formula for the width in terms of $\overline{\mathrm{MS}}$ masses and obtain

$$\begin{aligned} \Gamma(H \to b\bar{b}) = \Gamma_0 \bar{m}_b^2 \; & \left\{ 1 + \bar{x}_t \left(\frac{7}{2} + 3\ln\frac{M_H^2}{\bar{m}_t^2} \right) \right. \\ & \left. + \frac{\alpha_s}{\pi} \bar{x}_t \left(\frac{175}{6} - 12\zeta(2) + 26\ln\frac{M_H^2}{\bar{m}_t^2} + 3\ln^2\frac{M_H^2}{\bar{m}_t^2} \right) \right\}. \end{aligned} \tag{24}$$

Notice that the transformation of Eq.(23) implies that the first order QCD corrections $\Gamma_0 M_b^2(\alpha_s/\pi)[3 - 2\ln(M_H^2/M_b^2)]$ give rise to a contribution of order $\mathcal{O}(\alpha_s G_F \bar{m}_t^2)$ as well. Based on the given values for the pole masses the corresponding running masses amount to $\bar{m}_b = 2.84/2.69$ GeV and $\bar{m}_t = 179.44/170.04$ GeV for $M_H = 70/130$ GeV. In Figure 4 we plot the corrections of orders $G_F m_t^2$ and $G_F m_t^2 + \alpha_s G_F m_t^2$ according to Eqs.(23) and (24). The curves are strongly characterized by the linear rise in M_H due to the overall factor. For the on-shell result the QCD screening of the leading electroweak corrections is clearly visible. The $\overline{\mathrm{MS}}$ curves indicate that the two loop contribution is less important than for the OS scheme and suggest a better convergence behaviour of the perturbation series.

An inspection of Eq.(24) reveals that all large logarithms $\ln(M_H^2/M_b^2)$ have dropped out. Their absorption into the running bottom mass favours the use of the $\overline{\mathrm{MS}}$ mass over the OS-mass. There is no such strong preferance with respect to the top mass, considering that the scales of the Higgs and the top are not as far apart as the Higgs and the bottom scales. Corresponding logarithms $\ln(M_H^2/M_t^2)$ therefore cannot be considered as particularly dangerous. Instead one might tend to use the top pole mass as a quantity which is by definition more feasible in experiments. In this case the Higgs decay rate can be rewritten into the following form

$$\begin{aligned}\Gamma(H\to b\bar{b}) = \Gamma_0\bar{m}_b^2 \quad & \left\{1+\frac{17}{3}\frac{\alpha_s}{\pi}+X_t\left(\frac{7}{2}+3\ln\frac{M_H^2}{M_t^2}\right)\right. \\ & +\frac{\alpha_s}{\pi}X_t\left(\frac{167}{6}-12\zeta(2)+17\ln\frac{M_H^2}{M_t^2}-3\ln^2\frac{M_H^2}{M_t^2}\right) \\ & +\left(\frac{\alpha_s}{\pi}\right)^2\left(30.717-\frac{2}{3}\ln\frac{M_H^2}{M_t^2}+\frac{1}{9}\ln^2\frac{M_H^2}{\bar{m}_b^2}\right) \\ & \left.+\mathcal{O}(\frac{\bar{m}_b^2}{M_H^2})+\mathcal{O}(\alpha_s^2\frac{M_H^2}{M_t^2})\right\}.\end{aligned} \tag{25}$$

Several groups have contributed to the calculation of QCD corrections which we have included in the formula in first [13, 14, 27, 28, 29] and massless second order [30, 31]. Quadratic bottom mass corrections in second order [16, 33] and top quark contributions [32, 33, 34] are also available. We have not written these pieces into Eq.(25), but included them in our numerical analysis.

As was noticed in [33] the logarithms $\alpha_s^2\ln^2(M_H^2/\bar{m}_b^2)$ originate from flavour singlet type diagrams. They are not present in the rate for the decay into hadrons, but are introduced when the pure gluonic channel is subtracted. In Figure 5 the contributions coming from the orders $\alpha_s, \alpha_s^2, G_F M_t^2, \alpha_s G_F M_t^2$ are compared, normalized to the Born term $\Gamma_{\mathrm{Born}} = \Gamma_0\bar{m}_b^2$. The electroweak corrections may carry different sign depending on the Higgs mass. However, as compared to the QCD corrections, where the first order contributes about 20% and the second order about 5% to the corrections, the electroweak contributions are small. With $\mathcal{O}(G_F M_t^2) = -6.6/5.4$ per mille and $\mathcal{O}(\alpha_s G_F M_t^2) = -4.3/-3.9$ per mille for $M_H = 70/130$ GeV these effects become relevant for high precision experiments at the percent level.

Acknowledgments

We would like to thank K.G.Chetyrkin and J.H.Kühn for helpful discussions. A.K. thanks the Deutsche Forschungsgemeinschaft for financial support (grant Kw 8/1-1). Partial support by US DOE under Contract DE-AC03-76SF00098 is gratefully acknowledged.

A Appendix

The result from [9] for the relation between the pole mass and the bare mass of the bottom quark according to Eq.(2) is reproduced below. For convenient use in Section 2 the bare masses in Σ_S^0 and Σ_V^0 are already transformed into the $\overline{\mathrm{MS}}$ renormalized ones.

$$
\begin{aligned}
M_b = \; & m_0 \Bigg\{ 1 + \frac{\alpha_s}{\pi} \left(\frac{1}{\epsilon} + \frac{4}{3} + \ln \frac{\mu^2}{\bar{m}_b^2} + \epsilon \left[\frac{8}{3} + \frac{1}{2}\zeta(2) + \frac{4}{3} \ln \frac{\mu^2}{\bar{m}_b^2} + \frac{1}{2} \ln^2 \frac{\mu^2}{\bar{m}_b^2} \right] \right) \\
& + \bar{x}_t \left(\frac{3}{2}\frac{1}{\epsilon} + \frac{5}{4} + \frac{3}{2} \ln \frac{\mu^2}{\bar{m}_t^2} + \epsilon \left[\frac{9}{8} + \frac{3}{4}\zeta(2) + \frac{5}{4} \ln \frac{\mu^2}{\bar{m}_t^2} + \frac{3}{4} \ln^2 \frac{\mu^2}{\bar{m}_t^2} \right] \right) \\
& + \frac{\alpha_s}{\pi} \bar{x}_t \Bigg(\frac{1}{\epsilon} \left[\frac{21}{4} + \frac{3}{2} \ln \frac{\mu^2}{\bar{m}_t^2} + \frac{3}{2} \ln \frac{\mu^2}{\bar{m}_b^2} \right] \\
& \quad + \frac{77}{8} - \frac{5}{2}\zeta(2) + \frac{15}{4} \ln \frac{\mu^2}{\bar{m}_t^2} + \frac{13}{4} \ln \frac{\mu^2}{\bar{m}_b^2} \\
& \quad + \frac{9}{4} \ln^2 \frac{\mu^2}{\bar{m}_t^2} + \frac{3}{4} \ln^2 \frac{\mu^2}{\bar{m}_b^2} + \frac{3}{2} \ln \frac{\mu^2}{\bar{m}_t^2} \ln \frac{\mu^2}{\bar{m}_b^2} \Bigg) \Bigg\}
\end{aligned}
\tag{26}
$$

The overall counterterms are given for the different diagrams:

$$
\begin{aligned}
\bar{\Sigma}_S^{CT}(QCD) &= \frac{\alpha_s}{\pi}\frac{1}{\epsilon}\left(-1 - \frac{1}{3}\xi_s\right) \\
\bar{\Sigma}_V^{CT}(QCD) &= \frac{\alpha_s}{\pi}\frac{1}{\epsilon}\frac{1}{3}\xi_s \\
\bar{\Sigma}_S^{CT}(EW) &= \bar{x}_t \frac{-2}{\epsilon} \\
\bar{\Sigma}_V^{CT}(EW) &= \bar{x}_t \frac{1}{2\epsilon}
\end{aligned}
\tag{27}
$$

$$
\begin{aligned}
\bar{\Sigma}_S^{CT}(\mathrm{IN}) &= \frac{\alpha_s}{\pi}\bar{x}_t \left\{ \frac{1}{\epsilon^2}\left(1 - \frac{1}{3}\xi_s\right) + \frac{1}{\epsilon}\left(-\frac{1}{3} - \frac{1}{3}\xi_s\right) \right\} \\
\bar{\Sigma}_V^{CT}(\mathrm{IN}) &= \frac{\alpha_s}{\pi}\bar{x}_t \left\{ \frac{1}{\epsilon^2}\frac{1}{12}\xi_s + \frac{1}{\epsilon}\frac{1}{24}\xi_s \right\}
\end{aligned}
\tag{28}
$$

$$
\begin{aligned}
\bar{\Sigma}_S^{CT}(\mathrm{OUT}) &= \frac{\alpha_s}{\pi}\bar{x}_t \left\{ \frac{1}{\epsilon^2}\left(\frac{1}{2} + \frac{1}{6}\xi_s\right) + \frac{1}{\epsilon}\left(-\frac{5}{6} - \frac{1}{6}\xi_s\right) \right\} \\
\bar{\Sigma}_V^{CT}(\mathrm{OUT}) &= \frac{\alpha_s}{\pi}\bar{x}_t \left\{ \frac{1}{\epsilon^2}\frac{1}{12}\xi_s + \frac{1}{\epsilon}\left(-\frac{1}{8}\xi_s\right) \right\}
\end{aligned}
\tag{29}
$$

$$
\begin{aligned}
\bar{\Sigma}_S^{CT}(\mathrm{LEFT}) &= \frac{\alpha_s}{\pi}\bar{x}_t \left\{ \frac{1}{\epsilon^2}\left(\frac{5}{2} + \frac{5}{6}\xi_s\right) + \frac{1}{\epsilon}\left(-\frac{1}{2} + \frac{1}{2}\xi_s\right) \right\} \\
\bar{\Sigma}_V^{CT}(\mathrm{LEFT}) &= \frac{\alpha_s}{\pi}\bar{x}_t \left\{ \frac{1}{\epsilon^2}\left(-\frac{1}{2} - \frac{1}{3}\xi_s\right) + \frac{1}{\epsilon}\left(-\frac{1}{3} + \frac{1}{12}\xi_s\right) \right\}
\end{aligned}
\tag{30}
$$

The finite parts of the one and two loop contributions read as follows:

$$\begin{aligned}\bar{\Sigma}_S^{fin}(1-\text{loop}) = & \frac{\alpha_s}{\pi}\left\{-\frac{4}{3}-\frac{2}{3}\xi_s+\left(-1-\frac{1}{3}\xi_s\right)\ln\frac{\mu^2}{\bar{m}_b^2}\right\} \\ & +\bar{x}_t\left\{-2-2\ln\frac{\mu^2}{\bar{m}_t^2}\right\}\end{aligned} \tag{31}$$

$$\begin{aligned}\bar{\Sigma}_V^{fin}(1-\text{loop}) = & \frac{\alpha_s}{\pi}\left\{\frac{2}{3}\xi_s+\frac{1}{3}\xi_s\ln\frac{\mu^2}{\bar{m}_b^2}\right\} \\ & +\bar{x}_t\left\{\frac{3}{4}+\frac{1}{2}\ln\frac{\mu^2}{\bar{m}_t^2}\right\}\end{aligned} \tag{32}$$

$$\begin{aligned}\bar{\Sigma}_S^{fin}(2-\text{loop}) = \frac{\alpha_s}{\pi}\bar{x}_t & \left\{-\frac{37}{6}-\frac{1}{2}\xi_s+4\zeta(2)\right. \\ & +\left(-3-\frac{1}{3}\xi_s\right)\ln\frac{\mu^2}{\bar{m}_t^2}+\left(-2-\frac{2}{3}\xi_s\right)\ln\frac{\mu^2}{\bar{m}_b^2} \\ & \left.-2\ln^2\frac{\mu^2}{\bar{m}_t^2}+\left(-2-\frac{2}{3}\xi_s\right)\ln\frac{\mu^2}{\bar{m}_t^2}\ln\frac{\mu^2}{\bar{m}_b^2}\right\}\end{aligned} \tag{33}$$

$$\begin{aligned}\bar{\Sigma}_V^{fin}(2-\text{loop}) = \frac{\alpha_s}{\pi}\bar{x}_t & \left\{\frac{2}{3}-\frac{1}{3}\xi_s+\frac{1}{4}\xi_s\ln\frac{\mu^2}{\bar{m}_b^2}\right. \\ & +\left(-\frac{1}{6}-\frac{2}{3}\xi_s\right)\ln\frac{\mu^2}{\bar{m}_t^2} \\ & \left.+\frac{1}{2}\ln^2\frac{\mu^2}{\bar{m}_t^2}+\frac{1}{6}\xi_s\ln\frac{\mu^2}{\bar{m}_t^2}\ln\frac{\mu^2}{\bar{m}_b^2}\right\}\end{aligned} \tag{34}$$

References

[1] A. Olchevski, *Precision Tests of the Standard Model*, International Europhysics Conference on High Energy Physics, 27.7.–2.8.95, Brussels, Belgium.

[2] J.F. Gunion, H.E. Haber, G. Kane, S. Dawson, The Higgs Hunter's Guide, Addison Wesley 1990.

[3] B. Kniehl, Phys. Rep. 240 (1994) 211.

[4] D.Yu. Bardin, B.M. Vilenskii, P.Kh. Khristov, Sov. Journ. Nucl. Phys. 53 (1991) 152.

[5] B.A. Kniehl, Nucl. Phys. B 376 (1992) 3.

[6] A. Dabelstein, W. Hollik, Z. Phys. C 53 (1992) 507.

[7] B.A. Kniehl, A. Sirlin, Phys. Lett. B 318 (1993) 367.

[8] B.A. Kniehl, Phys. Rev. D 50 (1994) 3314.

[9] A. Kwiatkowski, M. Steinhauser, Phys. Lett. B 338 (1994) 66, Err. ibid. B 432 (1995) 455.

[10] B.A. Kniehl, M. Spira, Nucl. Phys. B 432 (1994) 39.

[11] B.A. Kniehl, M. Steinhauser, e-Print HEP-PH/9507382, July 1995, accepted for publication in Phys. Lett. B.

[12] B.A. Kniehl, M. Steinhauser, e-Print HEP-PH/9508241, August 1995, accepted for publication in Nucl.Phys.B.

[13] E. Braaten, J.P. Leveille, Phys. Rev. D 22 (1980) 715.

[14] N. Sakai, Phys. Rev. D 22 (1980) 2220.

[15] A.L. Kataev, V.T. Kim, Mod. Phys. Lett. A Vol. 9, No. 14 (1994) 1309.

[16] L.R. Surguladze, Phys. Lett. B 341 (1994) 60.

[17] R. Hempfling, B.A. Kniehl, Phys. Rev. D 51 (1995) 1386.

[18] G.B. Pivovarov, F.V. Tkachov, Preprint INR P-0370 (1984), Moscow;
F.V. Tkachov, Int. Journ. Mod. Phys. A 8 (1993) 2047;
G.B. Pivovarov, F.V. Tkachov, Int. Journ. Mod. Phys. A 8 (1993) 2241.

[19] S.G. Gorishny, S.A. Larin, Nucl. Phys. B 283 (1987) 452;
S.G. Gorishny, Nucl. Phys. B 319 (1989) 633.

[20] K.G. Chetyrkin,V.A. Smirnov, Preprint INR P-518 (1987), Moscow;
K.G. Chetyrkin, Preprint MPI-PAE/PTh 13/91 (1991), Munich;
V.A. Smirnov, Commun. Math. Phys. 134 (1990) 109.

[21] V.A. Smirnov, Renormalization and Asymptotic Expansion, (Birkhäuser, Basel, 1991).

[22] K.G. Chetyrkin, J.H Kühn, A. Kwiatkowski, *Reports of the Working Group on Precision Calculations for the Z Resonance*, CERN 95-03 Yellow Report, p. 175, eds. D. Bardin, W. Hollik, G. Passarino.

[23] S.A. Larin, F.V. Tkachov, J.A.M. Vermaseren, Preprint NIKHEF-H/91-18 (1991).

[24] J.A.M. Vermaseren, Symbolic Manipulation with FORM, Version 2, (Computer Algebra Netherlands Amsterdam, 1991).

[25] N. Gray, D.J. Broadhurst, W. Grafe, K. Schilcher, Z. Phys. C 48 (1990) 673.

[26] O. Nachtmann, W. Wetzel, Nucl. Phys. B 187 (1981) 333.

[27] T. Inami, T. Kubota, Nucl. Phys. B 179 (1981) 171.

[28] M. Drees, K. Hikasa, Phys. Rev. D 41 (1990) 1547; Phys. Lett. B 240 (1990) 455; erratum ibid. B 262 (1991) 497.

[29] L.R. Surguladze, F.V. Tkachov, Nucl. Phys. B 331 (1990) 35.

[30] S.G. Gorishny, A.L. Kataev, S.A. Larin, Sov. J. Nucl. Phys. 40 (1984) 329.

[31] S.G. Gorishny, A.L. Kataev, S.A. Larin, L.R. Surguladze, Mod. Phys. Lett. A 5 (1990) 2703; Phys. Rev. D 43 (1991) 1633.

[32] B.A. Kniehl, Phys. Lett. B 343 (1995) 299.

[33] K.G. Chetyrkin, A.Kwiatkowski, Preprint TTP 95–23, LBL-37269, HEP-PH/9505358, May 1995.

[34] S.A. Larin, T. van Ritbergen, J.A.M. Vermaseren, Preprint NIKHEF-H/95-027, HEP-PH/9506465, June 1995.

Figure Captions

Figure 1: Order $\mathcal{O}(\alpha_s G_F M_t^2)$ self energy diagrams for the bottom quark. Thin line: bottom quark, thick line: top quark, curly line: gluon, dashed line: Higgs ghost.

Figure 2: Counterterm diagrams up to order $\mathcal{O}(\alpha_s G_F M_t^2)$,

Figure 3: Finite terms for diagrams up to order $\mathcal{O}(\alpha_s G_F M_t^2)$.

Figure 4: Corrections to $\Gamma(H \to b\bar{b})$ in terms of pole masses (upper curves) and $\overline{\mathrm{MS}}$ masses (lower curves). The solid lines are the $\mathcal{O}(G_F m_t^2)$ contributions and the dashed lines the sum of $\mathcal{O}(G_F m_t^2)$ and $\mathcal{O}(\alpha_s G_F m_t^2)$.

Figure 5: Corrections $\Gamma(H \to b\bar{b})$ separately for the orders $\mathcal{O}(\alpha_s)$ (solid curve), $\mathcal{O}(\alpha_s^2)$ (dashed-dotted curve), $\mathcal{O}(G_F M_t^2)$ (dashed curve) and $\mathcal{O}(\alpha_s G_F M_t^2)$ (dotted curve).

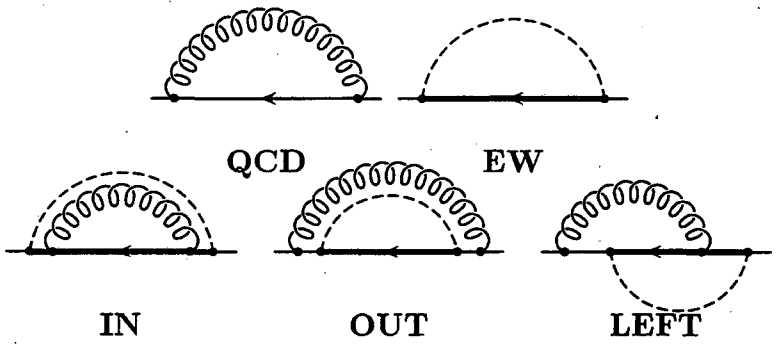

Figure 1

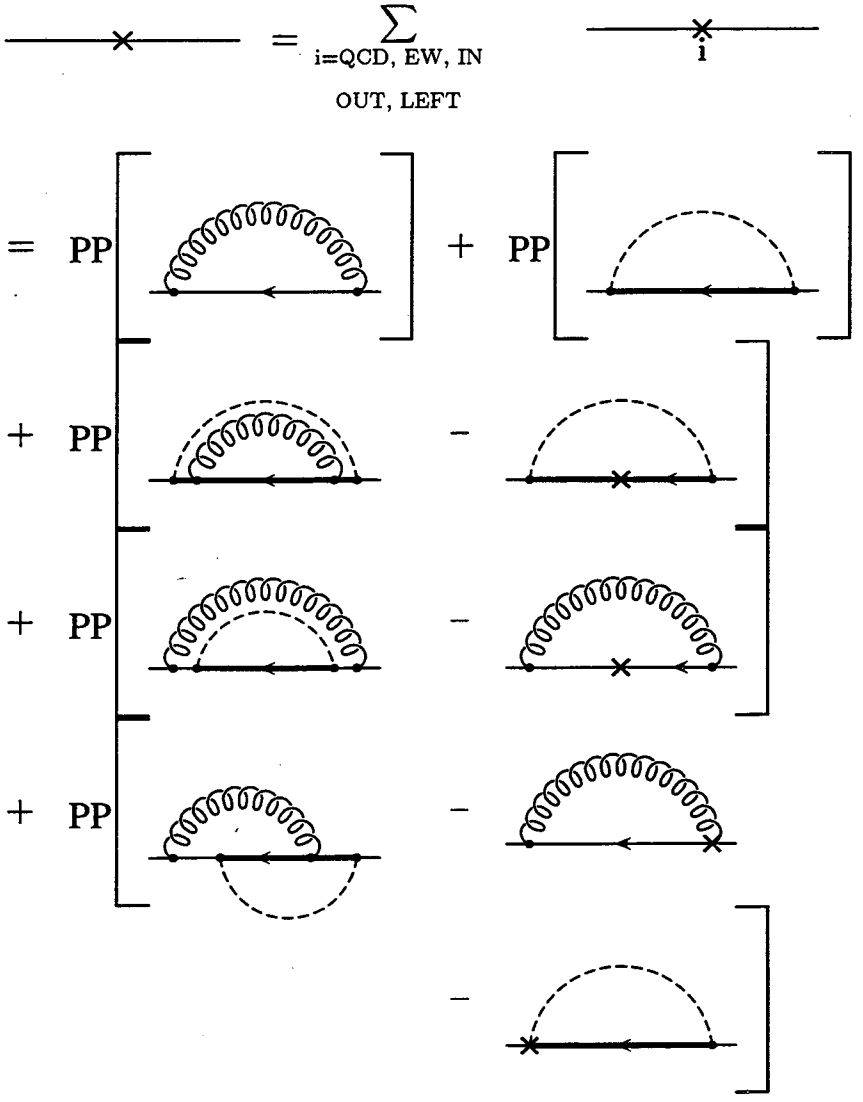

Figure 2

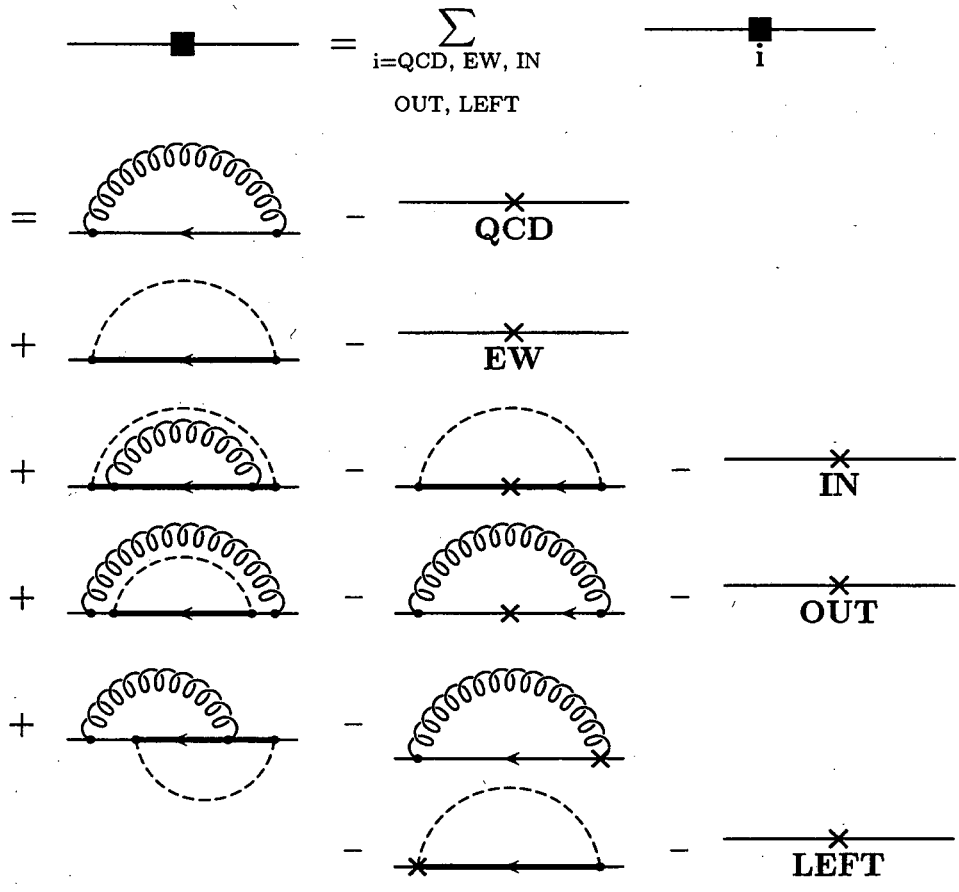

Figure 3

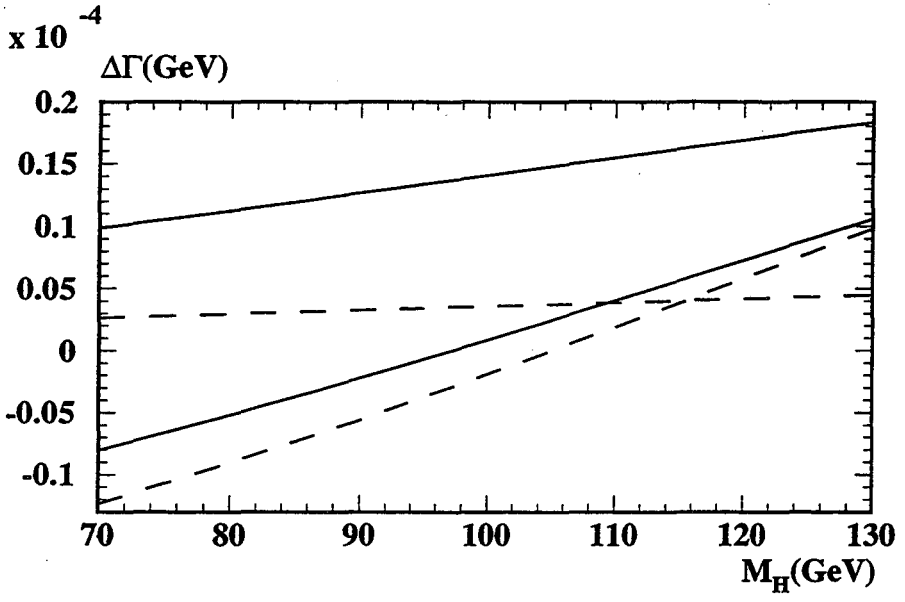

Figure 4

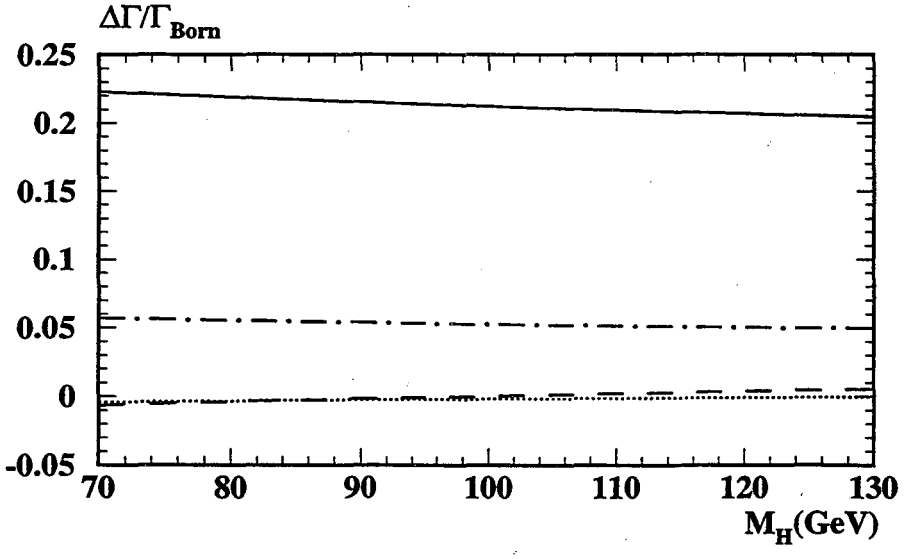

Figure 5

LAWRENCE BERKELEY NATIONAL LABORATORY
UNIVERSITY OF CALIFORNIA
TECHNICAL & ELECTRONIC INFORMATION DEPARTMENT
BERKELEY, CALIFORNIA 94720